Research Article Open Access

Santi Pailoplee*

Probabilities of Earthquake Occurrences along the Sumatra-Andaman Subduction Zone

DOI 10.1515/geo-2017-0004
Received May 11, 2015; accepted August 21, 2015

Abstract: Earthquake activities along the Sumatra-Andaman Subduction Zone (SASZ) were clarified using the derived frequency-magnitude distribution in terms of the (i) most probable maximum magnitudes, (ii) return periods and (iii) probabilities of earthquake occurrences. The northern segment of SASZ, along the western coast of Myanmar to southern Nicobar, was found to be capable of generating an earthquake of magnitude 6.1–6.4 M_w in the next 30–50 years, whilst the southern segment of offshore of the northwestern and western parts of Sumatra (defined as a high hazard region) had a short recurrence interval of 6-12 and 10-30 years for a 6.0 and 7.0 M_w magnitude earthquake, respectively, compared to the other regions. Throughout the area along the SASZ, there are 70– almost 100% probabilities of the earthquake with M_w up to 6.0 might be generated in the next 50 years whilst the northern segment had less than 50% chance of occurrence of a 7.0 M_w earthquake in the next 50 year. Although Rangoon was defined as the lowest hazard among the major city in the vicinity of SASZ, there is 90% chance of a 6.0 M_w earthquake in the next 50 years. Therefore, the effective mitigation plan of seismic hazard should be contributed.

Keywords: seismicity; frequency-magnitude distribution; recurrence interval; probability; Sumatra-Andaman Subduction Zone

1 Introduction

Among the tectonic plate boundaries, the Sumatra-Andaman Subduction Zone (SASZ; Kanamori, 2006) is one of the most active seismic source zones. Hazardous earthquakes occur frequently along the SASZ, even within the short period of a human lifespan. For instance based on the Global Centroid Moment Tensor (GCMT; http://www.globalcmt.org/CMTsearch.html) catalogue, 13 events of major earthquakes, M_w 7.0-7.9 were reported within the 38-year period from 1976–2014 (Fig. 1). Moreover during the last decade, 4 great earthquakes with $M_w \geq 8.0$ were posed in this region including the devastating M_w 9.0 earthquake on December 26th, 2004. Consequently, a large number of researchers have attempted to evaluate the earthquake hazards along the SASZ.

Nuannin et al. (2005) investigated the consistency between the b-value of the frequency-magnitude distribution (FMD) (Ishimoto and Iida, 1939; Gutenberg and Richter, 1944) and the characteristic of the M_w 9.0 earthquake. Using suitable empirical assumptions with the preceding seismicity data, the spatial distribution of the comparatively low b-values were found to agree quite well with the rupture area of the subsequent M_w 9.0 earthquake (Nuannin et al., 2005). In addition, they also concluded that the variations in b-value of the FMD can be used for earthquake prediction.

Thereafter, Pailoplee et al. (2013) evaluated the low b-value areas along the northern segment of the SASZ according to the assumption of Nuannin et al. (2005) and from their results they proposed two prospective areas that are capable of generating earthquakes in the near future i.e., the northern offshore area of the Nicobar Islands and the western coast of Myanmar.

Similarly, Pailoplee and Choowong (2013) evaluated the earthquake activities for the bulk of SASZ region. The most probable maximum magnitudes, and recurrence intervals, including the probabilities of earthquake occurrence, were estimated approximately using the FMD analyzed from the seismicity data. However, in practice the coverage and reliability of the seismotectonic data is heterogeneous, in particular for the 4,000-km long SASZ. The epicentral earthquake distributions (Fig. 1) illustrate the difference in the seismicity values that are strongly active in some places whereas other areas are quiescent. Therefore, a detailed evaluation of the earthquake activities are needed which is the main aim of this study. The obtained results should be useful for preparing long-term mitiga-

***Corresponding Author: Santi Pailoplee:** Morphology of Earth Surface and Advanced Geohazards in Southeast Asia Research Unit (MESA RU), Department of Geology, Faculty of Science, Chulalongkorn University, Bangkok 10330, Thailand,
E-mail: Pailoplee.S@gmail.com; Tel.: (66) 2218-5456; Fax: (66) 2218-5456

tion plans for both seismic and tsunami hazards along the coastal communities of the SASZ, and in particular for Tavoy city, southern Myanmar where the deep seaport is being developed (Fig. 1).

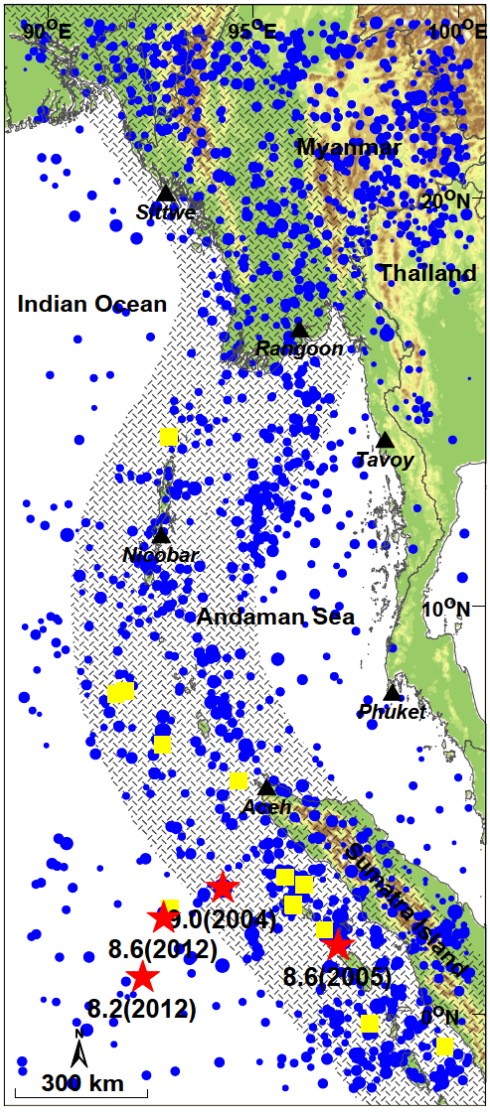

Figure 1: Map of the Sumatra-Andaman Subduction Zone (SASZ) (grey polygon) and the adjacent areas showing the epicentral distributions of the great earthquakes mentioned in the text (red stars, with M_w magnitude and year of occurrence) and the major earthquakes with a magnitude of ≥ 7.0 M_w (yellow squares) including all of the completeness main shocks reported during the period 1978-2012. The four principal cities that lie in the vicinity of the SASZ are shown (black triangles).

2 Dataset and completeness

Four data sets of earthquake catalogues compiled by (i) GCMT reported the earthquake data with the magnitude range 4.6-9.0 during 1976-2014, (ii) the Engdahl, van der Hilst and Buland Bulletin reported the earthquake data with the magnitude range 3.0-9.0 during 1960-2009 (EHB; http://www.isc.ac.uk/ehbbulletin), (iii) the International Seismological Centre reported the earthquake data with the magnitude range 1.5-9.0 during 1960-2012 (ISC; http://www.isc.ac.uk/), and (iv) the National Earthquake Information Center reported the earthquake data with the magnitude range 3.0-9.0 during 1979-2014 (NEIC; http://earthquake.usgs.gov/regional/neic/) were used as the primary sources for this study. The earthquakes with a focal depth beyond 40 km, defined as the intraslab earthquakes, were excluded in order to focus on the interplate activities of the SASZ.

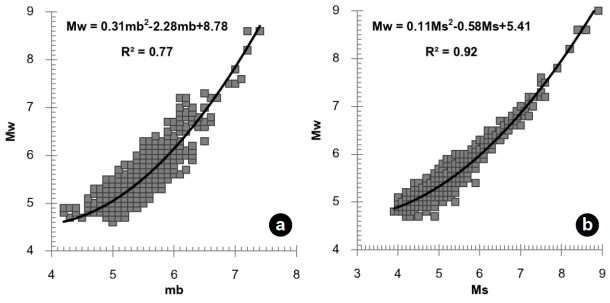

Figure 2: Empirical relationships between (a) M_w-m_b, and (b) M_w-M_s.

In order to homogenize the magnitude scales, the empirical relationships of M_w-m_b and M_w-M_s were contributed newly for the SASZ using the available GCMT catalogue (Fig. 2). According to the obtained relationships, m_b and M_s were converted to M_w which representing directly the physical properties of an earthquake source (Hanks and Kanamori, 1979). For M_L scale, the relationship between m_b and M_L proposed by Palasri and Ruangrassamee (2010) was applied., and then re-convert the obtained m_b to M_w using the M_w-m_b relationship proposed in this study.

Thereafter, earthquake declustering was performed according to the Gardner and Knopoff (1974) algorithm in order to screen the main shocks that directly represent the seismotectonic activities. As a result, around 2,974 earthquakes with a magnitude range of 2.0–9.0 M_w recorded during 1960–2014 were classified as the main shocks (Fig. 1).

Using the GENAS algorithm (Habermann, 1983; 1987) with the main shock dataset (obtained as above), the rates of the earthquake detection were found to be constant in terms of both the earthquake magnitude range 2.2–9.0 M_w and the time period 1978-2012 of recording. The essentially linear (straight line) increase in the cumulative numbers of earthquakes against time (Fig. 3a) supports that these earthquake dataset are not significantly impacted by any man-made changes, as recognized by Wyss (1991) and Zuniga and Wiemer (1999). Finally, the 1,960 main shocks reported during the 1978-2012 period with a magnitude range of 2.2–9.0 M_w are, therefore, defined as the meaningful earthquake dataset representing directly the seismotectonic activities of the SASZ and so are suitable for this statistical evaluation of earthquake activities.

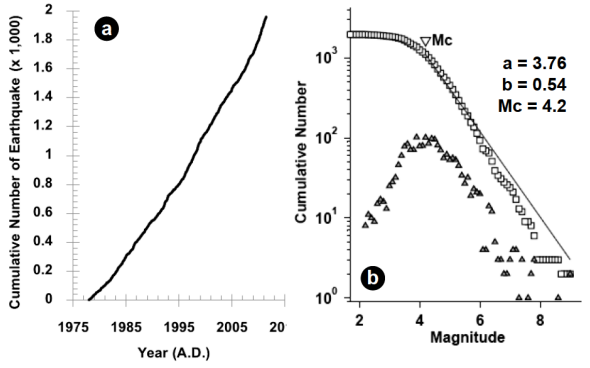

Figure 3: (a) Cumulative number of earthquakes after declustering and showing the constant rates of seismicity detected in the magnitude range 2.2–9.0 M_w during period 1978-2012. (b) FMD plot of the complete main shocks. Triangles indicate the number of earthquakes of each magnitude; squares represent the cumulative number of earthquakes equal to or larger than each magnitude. Solid lines are the lines of best fit according to Woessner and Wiemer (2005). Mc is defined as the magnitude of completeness.

3 Earthquake activity

The FMD (Ishimoto and Iida, 1939; Gutenberg and Richter, 1944) expresses the relationship between the occurrence rate per year (N) of earthquakes with magnitude ≥ M, as shown in Eq. (1);

$$\log(N) = a - bM, \text{ or } \ln(N) = \ln\alpha - \beta M \quad (1)$$

Empirically, the variables N and M are related together in terms of the linear regression, while the values of a and b are positive, real constants that vary depending on the specific space and time domain. From the seismological point of view, the a-value implies the entire seismicity rate whereas the b-value represents the ratio of the small-to-large earthquake occurrences. The values of α and β are related to a and b by Eqs. (2a) and (2b), respectively;

$$\alpha = \exp(a\ln(10)), \quad (2a)$$

and

$$\beta = b\ln(10) \quad (2b)$$

The FMD of the entire selected (complete) earthquake dataset was initially examined. From the linear regression plot of the FMD (Fig. 3b) the a- and b-values were estimated to be 3.76 and 0.54, respectively. By the entire-magnitude-range method (Woessner and Wiemer, 2005), the magnitude of completeness (Mc), representing the magnitude level of the complete report, was estimated to be 4.2 M_w.

To investigate in more detail, the SASZ was gridded with a 1° × 1° spacing. From the complete earthquake dataset, those within an empirically fixed 165-km radius of each grid node were selected and contributed to the FMD. The a- and b-values, standard deviation of b, Mc including percent of goodness fit, were evaluated simultaneously using the ZMAP program (Wiemer, 2001). The obtained values were then contoured and mapped, as illustrated in Fig. 4. In order to constrain the obtained maps, the FMD plots were examined for four areas (Fig. 5).

The spatial distributions of the a-values were all in the range of 1-5 (Fig. 4a). Two prominent areas of high a-values (>4), implying high earthquake activities, were located at (i) northern part of Sittwe and (ii) eastern part of Nicobar Islands (see also Figs. 5a, b). In contrast for the offshore region of the northwestern and inland of the Sumatra Island, the calculated a-value was markedly low (<2) (see also Figs. 5c, d).

In the case of the b-value map (Fig. 4b), three pockets of comparatively low b-value areas (<0.8) could be defined, which consisted of (i) inland, (ii) northwestern and (iii) western parts of Sumatra Island. According to Mogi (1962), Scholz (1968), and Wyss (1973), the smaller the b-value the more stress that is accumulated and so the greater is the earthquake magnitude that can be generated. Regardless of the a-values, the three low b-value areas mentioned above, therefore, imply a high possibility to generate a large magnitude earthquake surrounding the Sumatra territory. Based on the a- and b-value maps in Figs. 4a and b, the earthquake activities were then evaluated in terms of the most probable maximum magnitude (section 3.1), return period (section 3.2) and probability of occurrence (section 3.3).

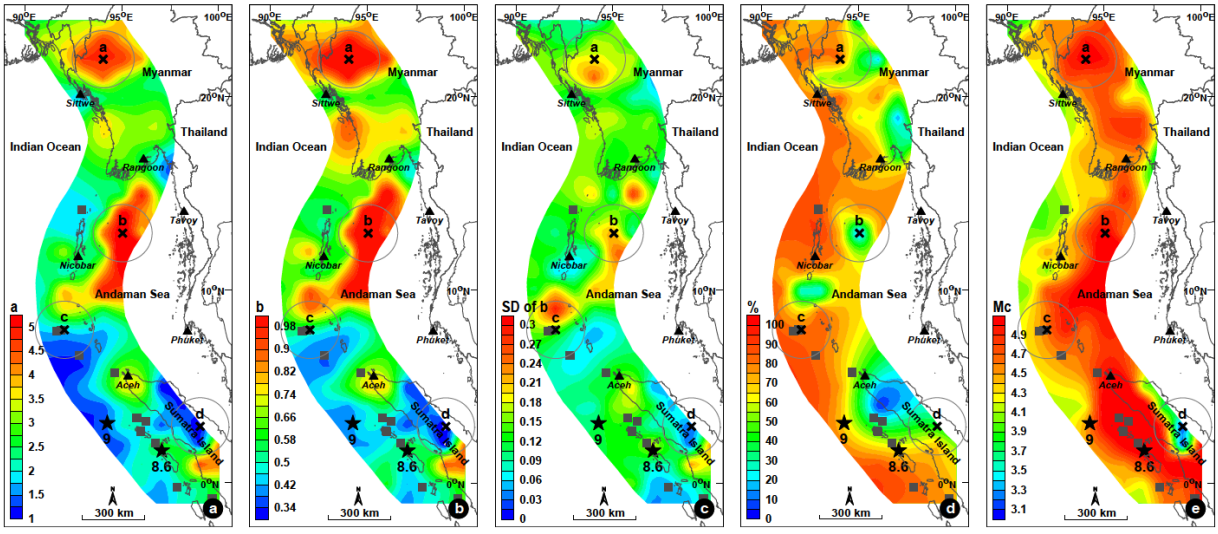

Figure 4: Spatial distributions of the (a) a-value, (b) b-value, (c) standard deviation of each obtained b-value, (d) the goodness fit of the FMD, and (e) magnitude of completeness.

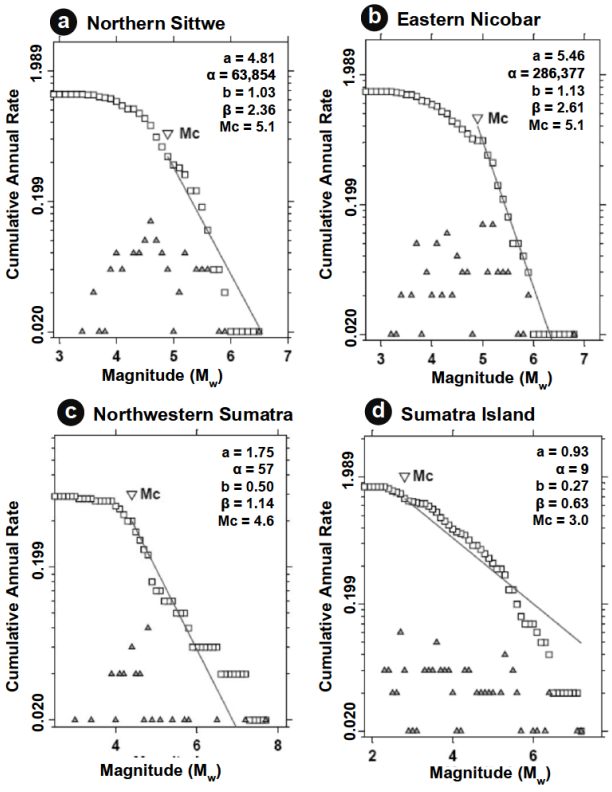

Figure 5: FMD plots of the earthquakes located within a 165-km radius from the four specific areas, a-d, shown in Fig. 4.

Regarding to the uncertainty of the calculated a- and b-values, Fig. 4c reveals the small areas of northern Sittwe, eastern and southern Nicobar depicting the high standard deviation of b-value. In addition, the goodness of fit (%), computing the difference between the observed FMD and a synthetic distribution, was also evaluated (Fig. 4d). According to Wiemer and Wyss (2000), the higher difference between observed FMD and a synthetic distribution leading to the lower goodness of fit. Based on Fig. 4d, it is illustrated that there are some small pockets illustrating low percent of goodness fit where mostly conform to those observed high standard deviation of b (Fig. 4c). This might be affected by the low limit of seismic detection along the SASZ as implied directly by the high value of Mc (Fig. 4e). Therefore, the regions showing high standard deviation and/or low percent of goodness fit mentioned above indicate the high statistical variation which should be careful in the seismic activity interpretation in the next section.

3.1 Most probable maximum magnitude

According to Yadav et al. (2011), various values representing the earthquake activities can be calculated using the α- and β- values from the FMD. For instance, the most probable maximum magnitude in the period of t years of interest (u_t) can be estimated as expressed in Eq. (3);

$$u_t = \frac{\ln(\alpha t)}{\beta}. \quad (3)$$

Thus, for each individual grid node, the a- and b-values obtained from the previous section were converted to the corresponding α- and β-values using Eqs. (2a) and (2b). The most probable maximum magnitude earthquake that could be generated in 5, 10, 30 and 50 years was then calculated and mapped (Fig. 6).

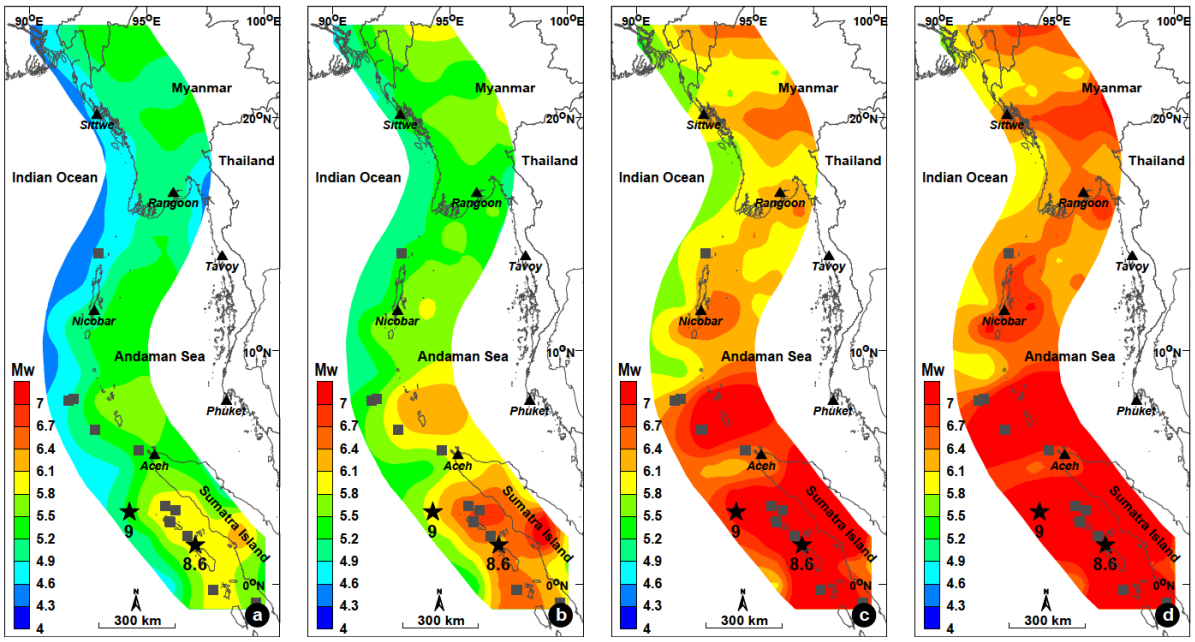

Figure 6: The probable maximum magnitude of earthquake capable of being generated in the individual time span of the next (a) 5, (b) 10, (c) 30, and (d) 50 years.

For instance in the next 5–10 year period (Figs. 6a, b), most areas are capable of generating an earthquake with a magnitude of around 4.6–5.2 M_w. Meanwhile for the northwestern and western Sumatra (close to the epicenter of M_w 9.0 and 8.6 earthquakes), these could likely generate an earthquake with a magnitude of 5.8–6.4 M_w.

With respect to the next 30- and 50-year periods (Figs. 6c, d), the west coast of Myanmar, and southern Nicobar, was found to have a possibility of generating an earthquake with a 6.1 and 6.4 M_w in the next 30- and 50-year periods, respectively. Meanwhile, the area surrounding the Sumatra Island was found to be capable of generating earthquakes with a magnitude of up to 7.0 M_w (Fig. 6d).

3.2 Earthquake return period

Using both the α- and β- parameters, the earthquake return period (T_M) in years for the considered earthquake magnitude M were evaluated using Eq. (4) (Yadav et al., 2011).

$$T_M = \frac{\exp(\beta M)}{\alpha} \tag{4}$$

The obtained recurrence maps illustrate various recurrence intervals depending on both the specific area and the recognized magnitude scale. Due to Kramer (1996) defined the M_w–4.0 earthquake as the lowest hazardous earthquake and Schwartz and Coppersmith, K.J. (1984) suggested that the earthquake with 7.0 M_w or greater mitht be acted as the characteristic earthquake, the recurrence inverval investigated here focuses in the magnitude range 4.0-7.0 M_w (Fig. 7). From this, two groups showing different hazard levels were segmented. For instance, in the offshore northwestern and western parts of Sumatra Island, defined as a high hazard region, the calculated recurrence intervals were found to be 1–3, 6–12, and 10–30 years for earthquakes of a magnitude of 5.0, 6.0 and 7.0 M_w, respectively. In contrast, for the low hazard area surrounding the northern part of west coast of Myanmar, and surrounding Nicobar Islands, the estimated recurrence intervals were 3-fold longer than the high hazard region, with a M_w 6.0 and 7.0 earthquake predicted to occur with an average return period of 20-30 and ≥ 100 years, respectively (Figs. 7c, d).

3.3 Probability of earthquake occurrence

The probabilities of earthquake occurrences, P_t (M), for any given specific time period (t) and certain magnitude (M) were also evaluated along the SASZ using Eq. (5).

$$P_t(M) = 1 - \exp(-\alpha t.\exp(-\beta M)) \tag{5}$$

The maps in Fig. 8 show the probabilities (%) that an earthquake of a magnitude within 4.0–7.0 M_w might occur in the next 50-year period. There are 70- almost 100% that the earthquakes with M_w up to 6.0 might be gener-

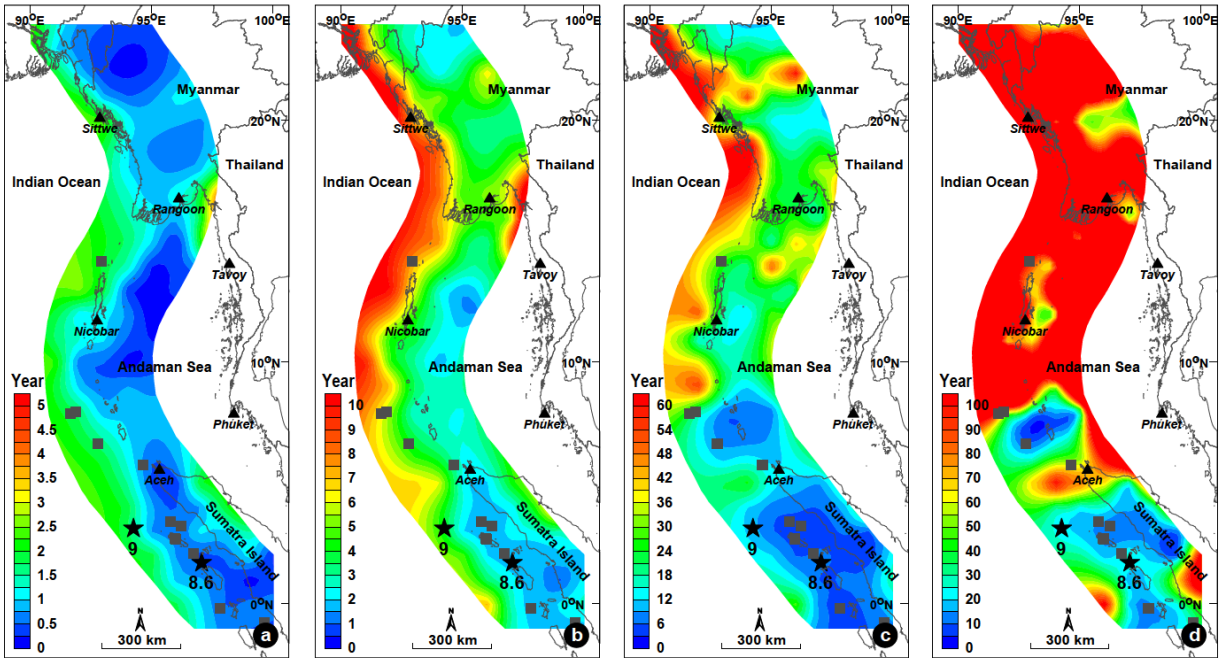

Figure 7: Return periods of earthquakes of magnitudes of (a) 4.0, (b) 5.0, (c) 6.0, and (d) 7.0 M_w.

ated throughout the SASZ (Figs. 8a, b, c). Meanwhilde for a 7.0 M_w earthquake, the probability of occurrence is less than 50% for the northern segment between the west coast of Myanmar to southern Nicobar, whereas it is still almost 100% for the southern segment surrounding the Sumatra Island that might be posed by the 7.0 M_w earthquake in the next 50 year (Fig. 8d).

In addition, for the four major cities located within the SASZ, the earthquake hazard curves, expressed in terms of the expected probability for an individual earthquake magnitude, are plotted in detail for time spans of the next 5, 10, 30 and 50 years (Fig. 9). From these hazard curves, it was clearly observed that probability of occurrence of an earthquake with a magnitude of ≥ 5.5 M_w in all recognized time spans decreases exponentially with the magnitude.

Among the four recognized cities, Rangoon (Fig. 9b), the previous capital city of Myanmar, had the lowest probability for an earthquake occurrence according to the SASZ, with a 20, 30, 70, and 90% probability of an earthquake of magnitude 6.0 M_w occurring in the next 5, 10, 30 and 50 years, respectively. Meanwhile, for the other three cities of Sittwe, Nicobar, and Aceh (Figs. **??**a, c, d), the probabilities were similar with that for a 7.0 M_w earthquake being generated in 5, 10, 30, and 50 years being around 10, 20, 50, and 60%.

4 Discussion and conclusion

In this study, the present-day earthquake activities along the SASZ were investigated statistically. After improving the completeness of earthquake catalogue, the spatial variation of the a- and b-values according to the FMD were analyzed and mapped. Then, some earthquake hazard parameters were evaluated using the obtained a- and b-values.

For the most probable maximum magnitude in a given time period, most areas were found to be able to generate an earthquake with a magnitude of up to 4.6–5.2 M_w in a 5- and 10-year period. However, for the area surrounding Sumatra Island, earthquakes with a magnitude of 6.7 and 7.0 M_w may occur in the next 30 and 50 years, respectively. In the case of Sittwe city, which has been suggested to be an upcoming earthquake source (Pailoplee et al., 2013), the occurrence of a 7.0 M_w magnitude earthquake is also possible even in the next 50 years. Although Pailoplee et al. (2013) also proposed the offshore area of the northern part of the Nicobar Islands as another candidate seismic source of future earthquakes, the most probable maximum magnitude evaluated in this study was found to be less than 6.4 M_w for the next 50-year period.

The recurrence maps illustrate the variety of the recurrence intervals across the SASZ. The offshore area of the northwestern and western parts of Sumatra Island was de-

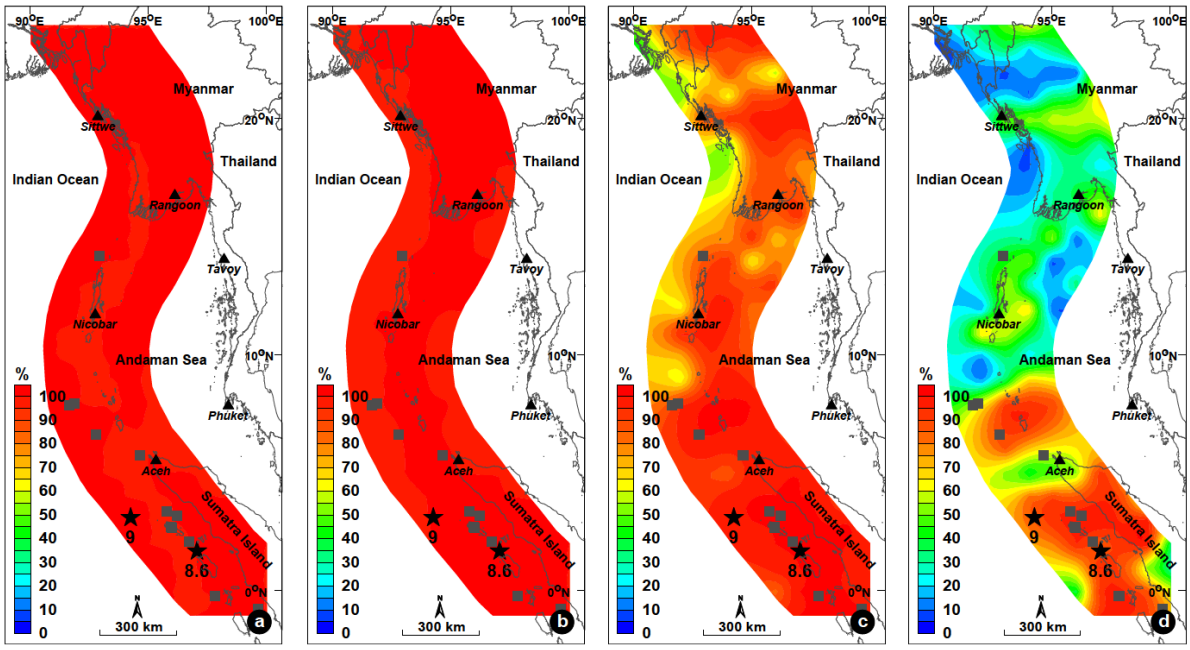

Figure 8: Probabilities of earthquake occurrences in a 50-year return period for different magnitudes of (a) 4.0, (b) 5.0, (c) 6.0, and (d) 7.0 M_W.

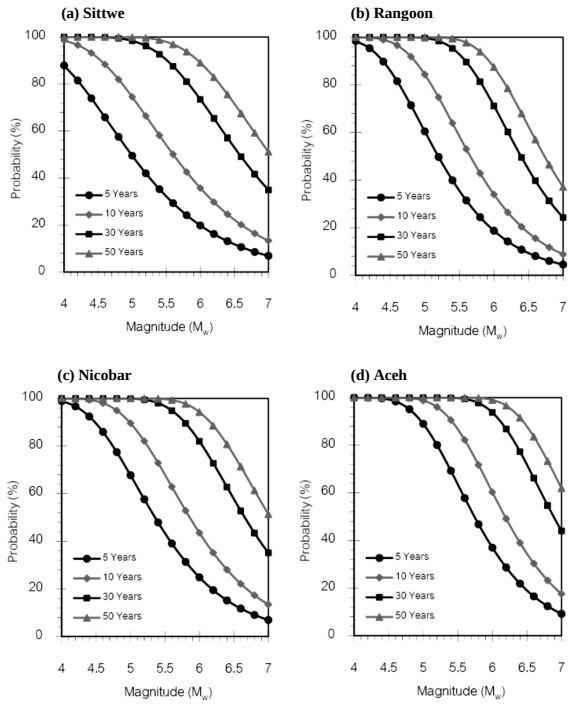

Figure 9: Probability of occurrence-magnitude curves for the four major cities located in the vicinity of the SASZ.

fined as a high hazard region with estimated recurrence intervals of around 1-30 years for an earthquake magnitude of 5.0-7.0 M_W. Meanwhile for the northern segment of western Myanmar-southern Nicobar Islands, the estimated recurrence interval was found to be up to 100 years for the occurrence of a 7.0 M_W earthquake.

For the probabilities of earthquake occurrence, there are 70-almost 100% that the earthquake with magnitude up to 6.0 M_W might occur along the SASZ in the next 50-year period. However in case of the M_W-7.0 earthquake, the northern segment of west coast of Myanmar-southern Nicobar Islands had a 10-50% probability of occurrence. Meanwhile for the southern segment recognized as high hazard areas, the probability that the M_W-7.0 earthquake might be generated in the next 50 year is more than 70%.

For the major cities within the SASZ, Rangoon city had the lowest probability for the occurrence of an earthquake, compared with the other cities, with the probability of generating an earthquake of 6.0 M_W in the next 5, 10, 30, and 50 years being 20, 30, 70, and almost 90%, respectively.

Acknowledgement: This research was supported by the Thailand Research Fund Grant for New Researchers (TRG5780152) and the ASEAN Studies Center, Chulalongkorn University. Thanks are also extended to T. Pailoplee for the preparation of the draft manuscript. I thank the Publication Counseling Unit (PCU), Faculty of Science, Chulalongkorn University, for a critical review and improved English. I acknowledge thoughtful comments and

suggestions by the editors and anonymous reviewers that enhanced the quality of this manuscript significantly.

References

Gardner, J.K.; Knopoff, L. (1974). Is the sequence of earthquakes in Southern California, with aftershocks removed, Poissonian?. Bulletin of the Seismological Society of America, 64(1), 363–367.

Gutenberg, B.; Richter, C.F. (1944). Frequency of earthquakes in California. Bulletin of the Seismological Society of America, 34, 185-188.

Habermann, R.E. (1983). Teleseismic detection in the Aleutian Island Arc. Journal of Geophysical Research, 88, 5056-5064.

Habermann, R.E. (1987). Man-made changes of Seismicity rates. Bulletin of the Seismological Society of America, 77, 141-159.

Hanks, T.C.; Kanamori, H. (1979). A moment-magnitude scale. Journal of Geophysical Research, 84, 2348-2350.

Ishimoto, M.; Iida, K. (1939). Observations of earthquakes registered with the microseismograph constructed recently. Bulletin of the Earthquake Research Institute, University of Tokyo, 17, 443-478.

Kanamori, H. (2006). Lessons from the 2004 Sumatra–Andaman earthquake. Philosophical Transactions of the Royal Society A: Mathematical, Physical and Engineering Sciences, 364, 1927-1945.

Kramer, S.L. (1996). Geotechnical Earthquake Engineering, Prentice Hall, Inc., Upper Saddle River, New Jersey.

Mogi, K. (1962). Magnitude frequency relations for elastic shocks accompanying fractures of various materials and some related problems in earthquakes. Bulletin of the Earthquake Research Institute, University of Tokyo, 40, 831–853.

Monecke, K.; Finger, W.; Klarer, D.; Kongko, W.; McAdoo, B.G.; Moore, A.L.; Sudrajat, S.U. (2008). A 1,000-year sediment record of tsunami recurrence in northern Sumatra. Nature, 455, 1232-1234.

Natawidjaja, D.H.; Sieh K.; Chlieh, M.; Galetzka, J.; Suwargadi, B.W.; Cheng, H.; Edwards, R.L.; Avouac, J.–P.; Ward, S.N. (2006). Source parameters of the great Sumatran megathrust earthquakes of 1797 and 1833 inferred from coral microatolls. Journal of Geophysical Research, 111, B06403-1-37.

Nuannin, P.; Kulhánek, O.; Persson, L. (2005). Spatial and temporal b-value anomalies preceding the devastating off coast of NW Sumatra earthquake of December 26, 2004. Geophysical Research Letters, 32, L11307.

Pailoplee, S.; Choowong, M. (2013). Probabilities of earthquake occurrences in Mainland South East Asia. Arabian Journal of Geoscience, 6, 4993–5006.

Pailoplee, S.; Surakiatchai, P.; Charusiri, P. (2013). b-value anomalies along the northern segment of Sumatra-Andaman Subduction Zone: Implication for the upcoming earthquakes. Journal of Earthquake and Tsunami, 7(3), 1350030-1-8.

Palasri, C.; Ruangrassamee, A. (2010). Probabilistic seismic hazard maps of Thailand. Journal of Earthquake and Tsunami, 4(4), 369–386.

Scholz, C.H. (1968). The frequency-magnitude relation of microfracturing in rock and its relation to earthquakes. Bulletin of the Seismological Society of America, 58, 399-415.

Schwartz, D.P.; Coppersmith, K.J. (1984). Fault behavior and characteristic earthquakes: Examples from the Wasatch and San Andreas fault zones. Journal of Geophysical Research, 89, 5681–5698.

Wiemer, S. (2001) A software package to analyze seismicity: ZMAP. Seismological Research Letters, 72, 373-382.

Wiemer, S.; Wyss, M. (2000). Minimum magnitude of complete reporting in earthquake catalogs: examples from Alaska, the western United States, and Japan. Bulletin of the Seismological Society of America, 90, 859–869.

Woessner, J.; Wiemer, S. (2005). Assessing the quality of earthquake catalogues: estimating the magnitude of completeness and its uncertainty. Bulletin of the Seismological Society of America, 95(2), 684-698.

Wyss, M. (1973). Towards a physical understanding of the earthquake frequency distribution. Geophysical Journal of the Royal Astronomical Society, 31, 341-359.

Wyss, M. (1991). Reporting history of the central Aleutians seismograph network and the quiescence preceding the 1986 Andreanof Island earthquake. Bulletin of the Seismological Society of America, 81, 1231-1254.

Yadav, R.B.S.; Tripathi, J.N.; Shanker, D.; Rastogi, B.K.; Das, M.C.; Kumar, V. (2011). Probabilities for the occurrences of medium to large earthquakes in northeast India and adjoining region. Natural Hazards, 56, 145-167.

Zuniga, F.R.; Wiemer, S. (1999). Seismicity patterns: are they always related to natural causes? Pageoph, 155, 713-726.